

# Revisiting DIERS Two-Phase Methodology For Reactive Systems Twenty Years Later

**Hans K. Fauske**

Fauske & Associates, LLC

Burr Ridge, IL 60527

## ABSTRACT

*Building upon the original DIERS methodology presented twenty years ago, an easy to use design methodology for reactive vapor, gassy and hybrid systems has resulted that properly accounts for two-phase flow effects. The methodology is illustrated to be consistent with available experimental and incident information and examples of bad and good design practices are provided for vapor, gassy and hybrid systems.*

## 1. INTRODUCTION

The original DIERS program completed in the 1980s [1], concluded that unless flow regime characterization data are available for a given system under prototypic runaway relief conditions, a homogeneous liquid-gas mixture entering the vent line at the peak venting requirement must be considered in order to assure a safe emergency relief design. Since the definition of peak reactive condition in addition to the onset of two-phase flow became the key to safe venting, the DIERS methodology conveniently grouped runaway reaction into three generic classes

- Vapor Systems
- Gassy Systems
- Hybrid Systems

Since the completion of the original DIERS program, it has frequently been suggested that the methodology can be so complex and time-consuming that it may be beyond the capability of many facility operators. Further, it has also been argued that the DIERS procedure can be overly conservative, leading to impractical relief system designs. As discussed below, this especially appears to be the case for gassy and hybrid systems as data and experience have become available. As a result, a generalized design method requiring no knowledge of physical properties is shown to be consistent with available data and experience for vapor, gassy and hybrid systems.

## 2. VAPOR SYSTEMS

For this class the smallest vent size is generally obtained with all vapor venting evaluated at the selected relief set pressure. However, quoting the 1983 report [1]: "Consideration of modest overpressures during venting has the effect of substantially reducing the difference in vent size between two-phase and all vapor venting."

## 2.1 Overpressure Effect

The dramatic effect of allowing for overpressure upon the vent area considering two-phase venting is illustrated in Figure 1. The calculations represent styrene polymerization using the DIERS computer code SAFIRE [2] considering the three vessel flow regimes of Homogeneous, Bubbly and Churn-Turbulent reflecting increasing vapor disengagement. For a non-foamy system where the disengagement characteristics can be represented by the Churn-Turbulent regime, the calculations reveal that a vent area based upon all vapor venting evaluated at the relief set pressure provides an adequate vent by allowing for a modest overpressure.<sup>1</sup>

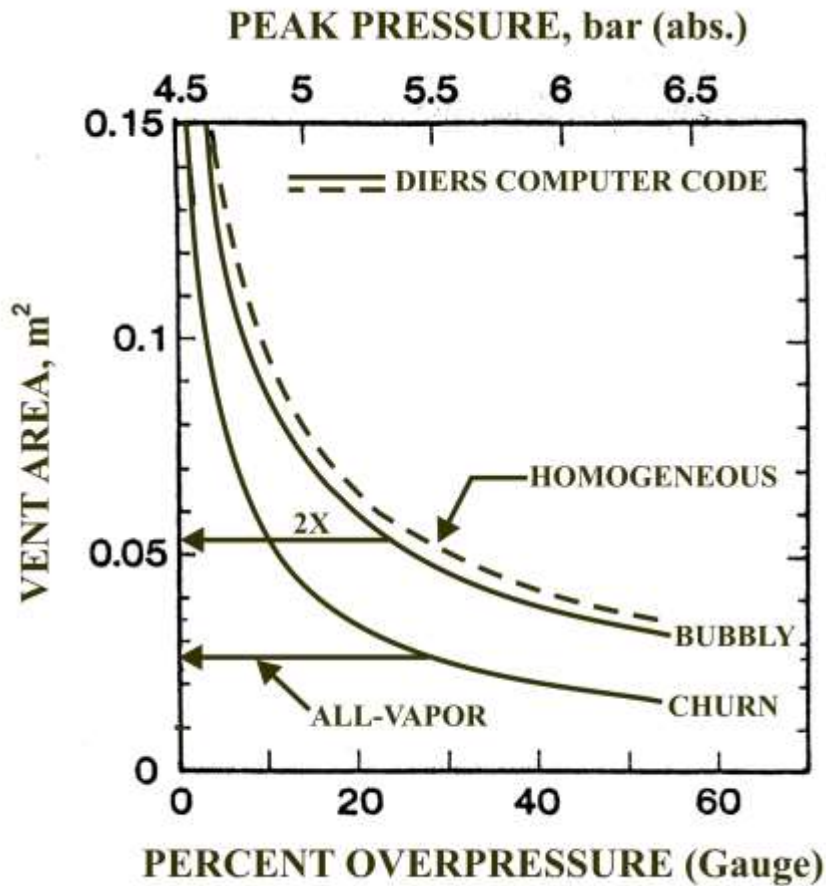


Figure 1. Dramatic Effect of Allowing for Overpressure

<sup>1</sup> It is of interest to note from Figure 1 that reactant loss due to two-phase flow can lead to vent areas smaller than that based on all vapor venting evaluated at the relief set pressure. As discussed later, this beneficial effect of two-phase flow is relevant to gassy and hybrid systems, where two-phase flow can occur well before reaching peak reactive conditions.

A conservative estimate of the all vapor vent area,  $A_v$  ( $m^2$ ), for critical flow is provided by

$$A_v = \frac{1}{0.61 C_D} \frac{m_o c \dot{T}}{\lambda P} \left( \frac{RT}{M_w} \right)^{1/2} \quad (1)$$

where

$C_D$  = discharge coefficient,  
 $m_o$  = mass of reactant,  
 $c$  ( $J\ kg^{-1}\ K^{-1}$ ) = specific heat,  
 $\dot{T}$  ( $^{\circ}C\ s^{-1}$ ) = self heat rate at relief set pressure,<sup>2</sup>  
 $\lambda$  ( $J\ kg^{-1}$ ) = latent heat of evaporation,  
 $P$  (Pa) = relief set pressure,  
 $R$  ( $8314\ Pa\cdot m^3/K\cdot kg\ mole$ ) = gas constant,  
 $T$  (K) = saturation temperature corresponding to  $P$ , and  
 $M_w$  ( $kg\ mole/mole$ ) = molecular weight.

For the styrene polymerization example illustrated in Figure 1,  $C_D = 1.0$ ,  $m_o = 9500\ kg$ ,  $c = 2470\ J\ kg^{-1}\ K^{-1}$ ,  $\dot{T} = 0.493\ K\ s^{-1}$ ,  $\lambda = 3.1 \times 10^5\ J\ kg^{-1}$ ,  $P = 4.5 \times 10^5\ Pa$ ,  $T = 482.5\ K$  and  $M_w = 106$ , and results in  $A_v = 0.0264\ m^2$ .

Figure 1 also reveals that for a foamy system where the disengagement characteristics can be represented by the bubbly or homogeneous vessel regimes, a vent area based upon twice that for all vapor venting would be adequate by again allowing for a modest overpressure.

The dramatic effect of the overpressure is also illustrated by the original DIERS two-phase simple design method for homogeneous two-phase vessel and vent line conditions

$$A_{TP} = \frac{1}{2 C_D} \frac{m_o \dot{T}}{(T/C)^{1/2} \Delta P} \quad (2)$$

or in terms of the dimensionless vent area ratio

$$\frac{A_{TP}}{A_v} = 0.3 \frac{\lambda}{T} \frac{P}{\Delta P} \left( \frac{M_w}{cR} \right)^{1/2} \quad (3)$$

where

$A_{TP}$  ( $m^2$ ) = vent area based on two-phase venting, and  
 $\Delta P$  (Pa) = overpressure.

Eq. 3 suggests that the ratio  $A_{TP} / A_v$  is inversely proportional to the overpressure  $\Delta P$ . Setting  $A_{TP} / A_v = 2.0$ , Eq. 3 leads to a modest overpressure of  $\Delta P = 9.9 \times 10^4\ Pa$ , or 22%

<sup>2</sup> DIERS developed a special bench-scale apparatus commercialized by Fauske & Associates, LLC as the Vent Sizing Package 2 VSP2<sup>TM</sup>. This adiabatic calorimeter is extensively used to obtain the value of  $\dot{T}$  corresponding to the relief set pressure.

overpressure based on an absolute basis or 28% overpressure on gauge basis, which is in excellent agreement with the DIERS SAFIRE computer code calculations illustrated in Figure 1.

The above observations which are generally applicable to vapor reactive systems can be restated as follows:

- The maximum penalty for not knowing the disengagement or flow regime characteristics is a vent area twice that based on all vapor venting,
- If the flow regime is known or can be determined to be non-foamy, the vent area can be based upon all vapor venting,
- Allowing for a modest overpressure represents a convenient and cost effective way to envelope uncertainties relating to two-phase flow regime and vapor disengagement characteristics, and
- Never size the vent area smaller than that required for all vapor venting.

In the case detailed knowledge of kinetics and necessary physical properties are lacking under the conditions of the emergency scenario (more often the case than not), the following simple design method requiring no knowledge of physical properties can be used which is consistent with the above observations based upon the original DIERS two-phase methodology [3]

$$A/V = \frac{C}{P \left[ 1 + \frac{1.98 \times 10^3}{P^{1.75}} \right]^{0.286}} \frac{\dot{T}}{C_D} \quad (4)$$

where

$A \text{ (m}^2\text{)} =$  vent area,

$V \text{ (m}^3\text{)} =$  volume of reactant,

$P \text{ (psig)} =$  relief set pressure,

$\dot{T} \text{ (}^\circ\text{C min}^{-1}\text{)} =$  self heat rate at relief set pressure,

$C_D =$  discharge coefficient,

$C = 3.5 \times 10^{-3}$  for churn turbulent or non-foamy system,

$C = 7.0 \times 10^{-3}$  for foamy or homogeneous like system.

Together with allowing for a modest over pressure of about 40% based on an absolute basis, Eq. 4 can be used to provide realistic vent sizing requirements as further illustrated in Table 1. Examples of both runaway experiences which vented safely and resulted in vessel ruptures are included.

## **2.2 Vapor System Design Example (ASME Coded Pressure Vessel)**

An example of bad and good design practices is illustrated in Table 2 for an atmospheric batch operation running away in a vessel with a MAWP = 20 psig. The bad practice illustrates the often common practice of setting the relief set pressure equal to the vessel MAWP. The allowable overpressure according to the code in this case is 10% of

Table 1. Comparison With Eq. 4

Source	A/V, m <sup>-1</sup>	P, psig	$\dot{T}$ , °C min <sup>-1</sup>	Eq. 4, A/V, m <sup>-1</sup>
DIERS-SAFIRE computer code Styrene; 40% overpressure Homogeneous, C <sub>D</sub> = 1.0	2.85 x 10 <sup>-3</sup>	51.1	29.6	2.95 x 10 <sup>-3</sup> (C = 7 x 10 <sup>-3</sup> )
DIERS-SAFIRE computer code Styrene; 40% overpressure Churn Turbulent, C <sub>D</sub> = 1.0	1.43 x 10 <sup>-3</sup>	51.1	29.6	1.48 x 10 <sup>-3</sup> (C = 3.5 x 10 <sup>-3</sup> )
DIERS 2.2 m <sup>3</sup> Styrene-ethylbenzene runaway test; Non-foamy; C <sub>D</sub> = 0.45	2.08 x 10 <sup>-3</sup>	64.8	21.6	2.03 x 10 <sup>-3</sup> (C = 3.5 x 10 <sup>-3</sup> )
Monsanto large-scale experience; Phenol-Formaldehyde runaway Foamy; C <sub>D</sub> = 0.5	9.0 x 10 <sup>-3</sup>	1.5	6.5	8.5 x 10 <sup>-3</sup> (C = 7.0 x 10 <sup>-3</sup> )
Phenol-Formaldehyde runaway experiment Foamy; C <sub>D</sub> = 0.5	2.8 x 10 <sup>-2</sup>	13	62	2.72 x 10 <sup>-2</sup>
6000 Gal industrial <u>incident</u> ; Phenol-Formaldehyde Foamy; C <sub>D</sub> = 0.5; Vessel ruptured	6.9 x 10 <sup>-3</sup>	4	50 (VSP simulation)	4 x 10 <sup>-2</sup> (C = 7.0 x 10 <sup>-3</sup> )
DuPont Chloroprene Runaway <u>Vented Safely</u> Foamy; C <sub>D</sub> = 0.6	7.1 x 10 <sup>-4</sup>	44	2.5	4.65 x 10 <sup>-4</sup> (C = 7.0 x 10 <sup>-3</sup> )
DuPont Chloroprene Runaway <u>incident</u> - vessel ruptured Foamy; C <sub>D</sub> = 0.6	1.07 x 10 <sup>-3</sup>	89	15	1.67 x 10 <sup>-3</sup> (C = 7 x 10 <sup>-3</sup> )
CHEERS 10.2 m <sup>3</sup> runaway methanol-acetic anhydride experiment, Non-foamy; C <sub>D</sub> = 1.0	2.21 x 10 <sup>-3</sup>	90.5	73	2.4 x 10 <sup>-3</sup> (C = 3.5 x 10 <sup>-3</sup> )

the gauge pressure (2 psi) but in terms of an absolute basis is only about 5.8%. Considering the batch is a typical phenol-formaldehyde system with a self heat rate,  $\dot{T}$ , of 30°C min<sup>-1</sup> at the relief set pressure of 20 psig, application of the DIERS two-phase methodology assuming homogeneous vessel conditions (Eq. 2) leads to a value of A/V of about 5.0 x 10<sup>-2</sup> m<sup>-1</sup>. Note that in Table 2, application of Eq. 4 is listed as not applicable (NA), since the allowable overpressure of about 5.8% falls well short of about 40% for the available overpressure required in order to apply Eq. 4.

Table 2. Example of Design Practices

Design Practice	Relief Set Pressure	% Overpressure Available	$\dot{T}$ , °C min	A/V (m <sup>-1</sup> ), Eq. 4
Bad	= MAWP = 20 psig	5.8	30	NA
Good	= 10 psig	48.6	20	5.0 x 10 <sup>-3</sup>

The good design practice illustrated in Table 2 uses a relief set pressure of 10 psig providing an available overpressure on an absolute basis of about 48.6%, i.e., in excess of that suggested for valid application of Eq. 4. Again considering homogeneous vessel conditions and a self heat rate of  $20^{\circ}\text{C min}^{-1}$  (as a result of the lower relief set pressure), application of Eq. 4 results in a value of  $A/V = 5.0 \times 10^{-3} \text{ m}^{-1}$ , which is consistent with the original DIERS two-phase methodology (Eq. 2) which results in  $5.6 \times 10^{-3} \text{ m}^{-1}$ . The order of magnitude decrease in the  $A/V$  value or the vent area  $A$ , by decreasing the relief set pressure from 20 psig (bad practice) to 10 psig (good practice) relates entirely to the corresponding increase in available overpressure from 5.8% to 48.6%. (It is noted that applying Eq. 4 with  $P = 20$  psig and  $\dot{T} = 30^{\circ}\text{C min}^{-1}$  results in  $A/V = 5.2 \times 10^{-3}$ , i.e. essentially the same results as obtained for the good practice case.)

In summary, the key to cost effective relief system designs for vapor reactive systems boils down to a proper selection of the relief set pressure well below the MAWP allowing at least an available overpressure of about 40% based upon an absolute basis. This practice should be possible in most cases dealing with ASME coded pressure vessels (design pressure  $\geq 15$  psig). Vent sizing requirement for low pressure storage tanks subjected to fire exposure and the resulting chemical reactivity where available overpressures on an absolute basis are much less than 40% is discussed below. Again, for non-foamy systems the methodology justifies relief sizing based upon all vapor venting to include a liquid-full vessel depending upon allowable overpressure relative to selected relief set pressure.

### **2.3 Low Pressure Reactive System Vapor Venting Methodology**

Given the absence of non-foamy characteristics, vapor venting requires a freeboard volume that is large enough to accommodate the liquid swell due to vapor formation and to subsequently prevent liquid entrainment.

#### **2.3.1 Liquid Swell**

In case of fire exposure, nucleation and bubble formation first occur at the heated wall. Based upon liquid swell measurements simulating fire exposure [4] and two-phase wall boundary layer analysis [5], the liquid swell  $\alpha_w$  can be represented by

$$\alpha_w \approx 5 \times 10^{-2} j_g / u_{\infty} \quad (5)$$

where  $j_g$  ( $\text{m s}^{-1}$ ) is the superficial vapor velocity and  $u_{\infty}$  ( $\text{m s}^{-1}$ ) is the characteristic bubble rise velocity. The equivalent expression for bulk boiling considering the churn-turbulent flow regime ( $\alpha_b \ll 1.0$ ) is

$$\alpha_b \approx \frac{1}{2} j_g / u_{\infty} \quad (6)$$

illustrating that

$$\alpha_w \ll \alpha_b \quad (7)$$

given the same vapor generation rate (i.e., same value of  $j_g / u_\infty$ ).

Further consideration of the bulk boiling analogy (where data indicate a rapid increase in vapor throughput at a void fraction of 0.5 which for churn-turbulent flow corresponds to a value of  $j_g / u_\infty$  of about 2) suggests that the liquid swell due to the two-phase wall boundary layer is limited to

$$\alpha_w \approx 0.1 \text{ for } j_g / u_\infty \geq 2 \quad (8)$$

Equation 8 implies the formation of wall two-phase continuous vapor boundary layer as the value of the ratio  $j_g / u_\infty$  exceeds 2 and is consistent with vented  $H_2O_2$  runaway reaction experiments [6]. The reported absence of two-phase flow is consistent with preferred wall nucleation and two-phase wall boundary layer formation with the corresponding liquid swell,  $\alpha_w$  not exceeding 0.1. The  $j_g / u_\infty$  ratio was about 13 [7].

The use of Eqs. 5 and 8 requires the absence of vapor generation throughout the bulk of the liquid and the liquid swell is due essentially to the wall boiling two-phase boundary layer associated with the fire heating. While the recirculation velocity ( $u_c$ ) resulting from the wall boiling two-phase boundary layer density effect can exceed the terminal bubble rise velocity ( $u_\infty$ ) which is typically of the order of  $0.2 \text{ m s}^{-1}$ , significant vapor carry-under and hence significant liquid swell, is prevented by static head effects. The increasing subcooling of the liquid as the vapor bubbles are dragged under by the recirculating flow results in rapid condensation and collapse of the vapor bubbles [4]. This behavior is confirmed by relevant fire simulation experiments and practical industry experience [4].

The above observation can be extended to include chemical heating as follows. Again, the absence of significant vapor generation throughout the bulk of the liquid is assured by the static head effect if the following inequality is satisfied

$$\dot{T}_{\text{chem}} < \phi \times u_c \quad (9)$$

where  $\dot{T}_{\text{chem}}$  ( $^{\circ}\text{C min}^{-1}$ ) is the chemical self-heat rate,  $\phi$  ( $^{\circ}\text{C m}^{-1}$ ) is the subcooled temperature gradient due to the liquid static head, and  $u_c$  ( $\text{m min}^{-1}$ ) is the average liquid recirculation velocity as a result of the wall boiling two-phase boundary layer density effect. Considering typical values for  $\phi$  and  $u_c$  of about  $2^{\circ}\text{C m}^{-1}$  and  $10 \text{ m min}^{-1}$ , respectively, chemical self-heat rates well below about  $20^{\circ}\text{C min}^{-1}$  should assure the absence of volumetric boiling as the bulk of the liquid will remain subcooled. As a result of the liquid recirculation, the sensible heating produced in the bulk liquid from the chemical reaction is largely transferred to the wall two-phase boundary layer in the form of latent heat.

The significance of the liquid swell being limited to the two-phase wall boundary layer is illustrated by considering a value of  $j_g / u_\infty$  equal to 4 resulting from the combined fire and chemical heating. For this example Eq. 8 suggests the liquid swell is limited to

10%. In contrast, considering bulk vapor formation and the churn-turbulent flow regime, the resulting liquid swell would be about 67%.<sup>3</sup>

### **2.3.2 Liquid Entrainment**

The necessary freeboard void fraction,  $\alpha_E$ , to prevent liquid entrainment into the vent line can be estimated from [8]

$$\alpha_E = \frac{d}{H} \left( \frac{u_o}{8 u_E} \right)^{1/2} \quad (10)$$

where  $d$  (m) is the vent diameter,  $H$  (m) is the vessel height,  $u_o$  ( $\text{m s}^{-1}$ ) is the inlet vapor velocity to the vent line and  $u_E$  ( $\text{m s}^{-1}$ ) is the entrainment velocity given by

$$u_E = 3 \left[ \frac{\sigma g \rho_\ell}{\rho_v^2} \right]^{1/4} \quad (11)$$

where  $\sigma$  ( $\text{kg s}^{-2}$ ) is the liquid surface tension,  $g$  ( $9.8 \text{ m s}^{-2}$ ) is the gravitational constant,  $\rho_\ell$  ( $\text{kg m}^{-3}$ ) is the liquid density and  $\rho_v$  ( $\text{kg m}^{-3}$ ) is the vapor density.

Typically the value of  $\alpha_E$  estimated from Eq. 10 for cases of interest is less than 0.05 or 5%. It follows from Eq. 8 that all vapor venting is assured if the initial freeboard,  $\alpha_F$ , at incipient boiling is about 15% or

$$\alpha_w + \alpha_E \leq \alpha_F \quad (12)$$

### **2.3.3 Two-Phase Venting**

If Ineq. 12 is not satisfied, a period of two-phase venting will persist prior to the onset of vapor venting. During this period, the pressure will increase relative to the relief set pressure if the vent size is based upon all vapor venting. Again if the overpressure resulting from two-phase flow does not exceed the allowable pressure, the relief design can be based upon all vapor venting even in the extreme case of liquid-full vessel conditions.

The time,  $t$  (s), to clear a vapor space to assure the onset of vapor venting can be estimated from

$$t = \frac{2 m_o (\alpha_E + \alpha_w) \lambda}{\dot{Q}_T (1 + G_\ell / G_v)} \quad (13)$$

---

<sup>3</sup> The churn-turbulent flow regime can be represented by  $j_g / u_\infty = 2\alpha/(1-\alpha)$ .



where  $m_o$  (kg) is the mass of the liquid-filled vessel,  $\lambda$  (J kg<sup>-1</sup>) is the latent heat of evaporation,  $\dot{Q}_T$  (J s<sup>-1</sup>) is the total heat input,  $G_L$  (kg m<sup>-2</sup> s<sup>-1</sup>) is the two-phase mass flux, and  $G_v$  (kg m<sup>-2</sup> s<sup>-1</sup>) is the vapor mass flux corresponding to all vapor venting.

Consistent with using the arithmetic average mass flux  $G = 1/2 (G_\ell + G_v)$  during the two-phase venting period, half the heat input from the fire and chemical reaction is considered to go into heating the liquid as sensible heat and results in the following overpressure  $\Delta P$  (Pa) before the onset of vapor venting

$$\Delta P = \frac{1}{2} \frac{\dot{Q}_T \lambda \rho_v}{m_o c T} t \quad (14)$$

where  $c$  (J kg<sup>-1</sup> K<sup>-1</sup>) is the liquid specific heat and  $T$  (K) is the liquid temperature. Substituting Eq. 13 into Eq. 14 results in

$$\Delta P = \frac{\lambda^2 \rho_v (\alpha_E + \alpha_w)}{(1 + G_\ell / G_v) c T} \quad (15)$$

### **2.3.4 Fire Simulation Experiment [4]**

It is of interest to check Eq. 15 against test conditions involving fire simulation ( $\dot{Q}_F = 5.2 \times 10^4$  J s<sup>-1</sup>) to a vertical vessel with  $D = 0.62$  m and  $H = 1.07$  m and initially filled with water. A short sharp entrance vent line with  $d = 2.54 \times 10^{-2}$  m resulted in an overpressure of about  $4.8 \times 10^3$  Pa (~ 0.7 psi) with the vent line initially open to the atmosphere. This observation is consistent with all vapor venting based upon a fire input  $\dot{Q}_F = 5.2 \times 10^4$  J s<sup>-1</sup> [7].

For this case the liquid swell fraction,  $\alpha_w$ , is provided by Eq. 5, since the ratio  $j_g / u_\infty$  is less than 2. The superficial velocity  $j_g$  is given by

$$j_g = \frac{4 \dot{Q}_F}{\lambda \rho_v \pi D^2} \quad (16)$$

and setting  $\lambda = 2.2 \times 10^6$  J kg<sup>-1</sup> and  $\rho_v = 0.6$  kg m<sup>-3</sup> results in  $j_g = 0.13$  m s<sup>-1</sup>. The relevant bubble rise velocity can be estimated from

$$u_\infty = 1.53 \left[ \frac{\sigma g}{\rho_\ell} \right]^{1/4} \quad (17)$$

where  $\sigma$  (0.06 kg s<sup>-2</sup>) is the water surface tension and  $\rho_\ell$  (950 kg m<sup>-3</sup>) is the saturated water density and results in  $u_\infty = 0.23$  m s<sup>-1</sup>. It follows from Eq. 5 that  $\alpha_w = 0.03$ .

The freeboard fraction,  $\alpha_E$ , to prevent liquid entrainment is provided by Eq. 10 and results in  $\alpha_E = 0.017$ , where  $u_o$  is estimated from

$$u_o = 0.61 (2 \Delta P / \rho_v)^{1/2} \quad (18)$$

and results in  $u_o = 80 \text{ m s}^{-1}$  and  $u_E$  is given by Eq. 11 and results in  $u_E = 18.8 \text{ m s}^{-1}$ .

The resulting overpressure  $\Delta P$  (Pa) due to initial two-phase flow is given by Eq. 15. The two-phase mass flux,  $G_\lambda$  ( $\text{kg m}^{-2} \text{ s}^{-1}$ ) is given by [9]

$$G_\ell = \rho_v \lambda (\text{TC})^{-1/2} \quad (19)$$

where  $T = 374 \text{ K}$ ,  $C = 4200 \text{ J kg}^{-1} \text{ K}^{-1}$  and results in  $G_\lambda = 1078 \text{ kg m}^{-2} \text{ s}^{-1}$ . The vapor mass flux,  $G_v$  ( $\text{kg m}^{-2} \text{ s}^{-1}$ ) is provided by

$$G_v = 0.61 (2 \Delta P \rho_v)^{1/2} \quad (20)$$

and with  $\Delta P = 4.8 \times 10^3 \text{ Pa}$  and  $\rho_v = 0.62 \text{ kg m}^{-3}$  results in  $G_v = 47 \text{ kg m}^{-2} \text{ s}^{-1}$ . Using these values in Eq. 15

$$\begin{aligned} \Delta P &= \frac{(22 \times 10^6)^2 (0.6) (0.03 + 0.017)}{(1 + 1078/47)(4200 \times 373)} \\ &= 3.8 \times 10^3 \text{ Pa or } \underline{0.56 \text{ psi}} \end{aligned}$$

which is less than the measured overpressure of about 0.7 psi which is the required value to support all vapor venting based upon a fire heat input of  $\dot{Q}_F = 5.2 \times 10^4 \text{ J s}^{-1}$ . Eq. 11 is therefore considered to be a reasonable representation of the overpressure resulting from two-phase flow prior to all vapor venting given a liquid-full vessel.

### **2.3.5 Low Pressure Design Example**

Consider an API-650 uninsulated vessel (12' diameter x 18' vertical on grade) with a 15000 gallon capacity containing styrene exposed to fire. The volumetric heating rate due to fire exposure is  $1.3^\circ\text{C min}^{-1}$ , the adiabatic chemical heating rate at a relief set pressure of 0.13 psig is  $1.9^\circ\text{C min}^{-1}$ , (note that this value is much smaller than that required by Ineq. 9), resulting in a combined heating rate of about  $3.2^\circ\text{C min}^{-1}$ . The maximum allowable venting pressure is 0.7 psig.

For this example, considering bulk volumetric boiling resulting in flashing two-phase venting (the DIERS methodology) requires a vent area of about  $2390 \text{ in}^2$  and allows for an overpressure of 0.57 psi. However, since Ineq. 9 is clearly satisfied and since the reacting styrene monomer is non-foamy (Figure 2), in this case the vent area can be estimated from Eq. 4.



Styrene, Non-Foamy



1000 ppm Soapy Water

Figure 2. Boiling Flow Regime Tests Comparison at Heating Rate of  $\sim 2^\circ\text{C min}^{-1}$

Setting  $V = 56.8 \text{ m}^3$ ,  $P = 0.13 \text{ psig}$  and  $\dot{T} = 3.2^\circ\text{C min}^{-1}$ , results in  $A = 0.2 \text{ m}^2$  or  $312 \text{ in}^2$ . Equation 4 is based upon all vapor venting and provides a practical approach to pressure relief evaluation for monomer storage tanks exposed to fire and undergoing chemical heating as well.<sup>4</sup> This is also the case for a styrene-full vessel since the pressure increase,  $\Delta P$ , due to early two-phase flow estimated from Eq. 15 is less than the available overpressure. Setting  $\lambda = 3.54 \times 10^5 \text{ J kg}^{-1}$ ,  $\rho_v = 3.05 \text{ kg m}^{-3}$ ,  $\alpha_E + \alpha_w \approx 0.15$ ,  $G_L = 1172 \text{ kg m}^{-2} \text{ s}^{-1}$ ,  $G_v = 78 \text{ kg m}^{-2} \text{ s}^{-1}$ ,  $c = 2175 \text{ J kg}^{-1} \text{ K}^{-1}$  and  $T = 418 \text{ K}$ , results in  $\Delta P = 3800 \text{ Pa}$  or  $0.55 \text{ psi}$  which compares to the available overpressure of  $0.57 \text{ psi}$ .

### **3. GASSY SYSTEMS**

In contrast to vapor systems, vent sizing based upon gas venting must coincide with peak volume generation rate, which can occur quite late in the venting period. Quoting the 1983 DIERS technology report [1] "in theory, therefore, early two-phase venting resulting in an appreciable loss of unreacted liquid can lead to a smaller vent size as compared to all gas venting."

However, in the absence of experimental gassy venting data at the time, the DIERS methodology suggested a conservative approach (worst case) by assuming two-phase homogeneous venting coinciding with the peak volume generation

$$A = \frac{\dot{Q}_{\max} \rho_\ell (1 - \alpha)}{G} \quad (21)$$

<sup>4</sup> Using actual styrene properties instead of Eq. 4 result in  $A = 0.197 \text{ m}^2$  based upon all vapor venting at the relief set pressure of  $0.13 \text{ psig}$ .

where

$A$  ( $\text{m}^2$ ) = vent area based on homogeneous two-phase flow,

$\dot{Q}_{\text{max}}$  ( $\text{m}^3 \text{s}^{-1}$ ) = peak gas volume generation rate,

$\rho_\ell$  ( $\text{kg m}^{-3}$ ) = reactant density,

$\alpha$  = the initial free board volume, and

$G$  ( $\text{kg m}^{-2} \text{s}^{-1}$ ) = homogeneous gas-liquid flow rate.

In this case the augmentation in vent size relative to gas venting is very large and is to the first order proportional to  $(\rho_\ell / \rho_g)^{1/2}$  where  $\rho_g$  ( $\text{kg m}^{-3}$ ) is the product gas density. In contrast to vapor systems, accounting for a modest overpressure at peak gas volume generation rate conditions will not significantly change this difference.

It is therefore of interest to note that gassy system experimental venting information is now available that support the theoretical suggestion that early two-phase venting can lead to a smaller vent size as compared to all gas venting [10].

The benefit from two-phase flow during the period prior to turnaround in peak venting pressure, is illustrated by evaluating the average vessel void fraction,  $\bar{\alpha}$ , corresponding to complete disengagement [10]

$$\frac{V(1-\bar{\alpha})\rho_\ell}{m_t} \frac{v\dot{P}}{P} = \frac{2\bar{\alpha}}{1-1.5\bar{\alpha}} u_\infty A_{\text{vessel}} \quad (22)$$

where

$V$  ( $\text{m}^3$ ) = volume of vessel,

$\rho_\ell$  ( $\text{kg m}^{-3}$ ) = reactant density,

$m_t$  ( $\text{kg}$ ) = RSST sample mass ( $\sim 0.01 \text{ kg}$ ),

$v$  ( $\text{m}^3$ ) = RSST containment volume ( $\sim 3.5 \times 10^{-4} \text{ m}^3$ ),

$\dot{P}$  ( $\text{psi s}^{-1}$ ) = peak rate of pressure rise in the RSST containment vessel,

$u_\infty$  ( $\text{m s}^{-1}$ ) = bubble rise velocity ( $\sim 0.2 \text{ m s}^{-1}$ ), and

$A_{\text{vessel}}$  ( $\text{m}^2$ ) = cross-sectional area of vessel.

Considering the RSST 37.5 wt% 3,5,5 Trimethyl Hexanoyl Peroxide data (Figure 3 with  $P \approx 1000 \text{ psi min}^{-1}$ ) and the corresponding 33  $\ell$  ( $V = 0.033 \text{ m}^3$  and  $A_{\text{vessel}} = 7.24 \cdot 10^{-2} \text{ m}^2$ ) venting tests (Figure 4), Eq. 22 provides the following value of  $\bar{\alpha}$  as a function of peak venting pressure  $P$ .

Table 3. Value of Disengagement Void Fraction,  $\bar{\alpha}$

P, psia	$\bar{\alpha}$
30	$\sim 0.61$
50	$\sim 0.59$
100	$\sim 0.55$
200	$\sim 0.49$
400	$\sim 0.40$

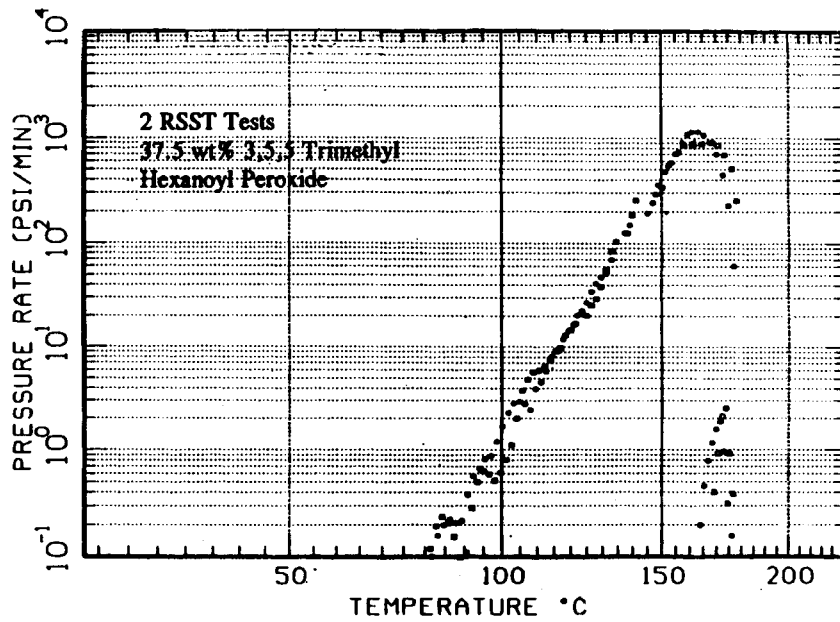


Figure 3. Peak Pressure Rate Data

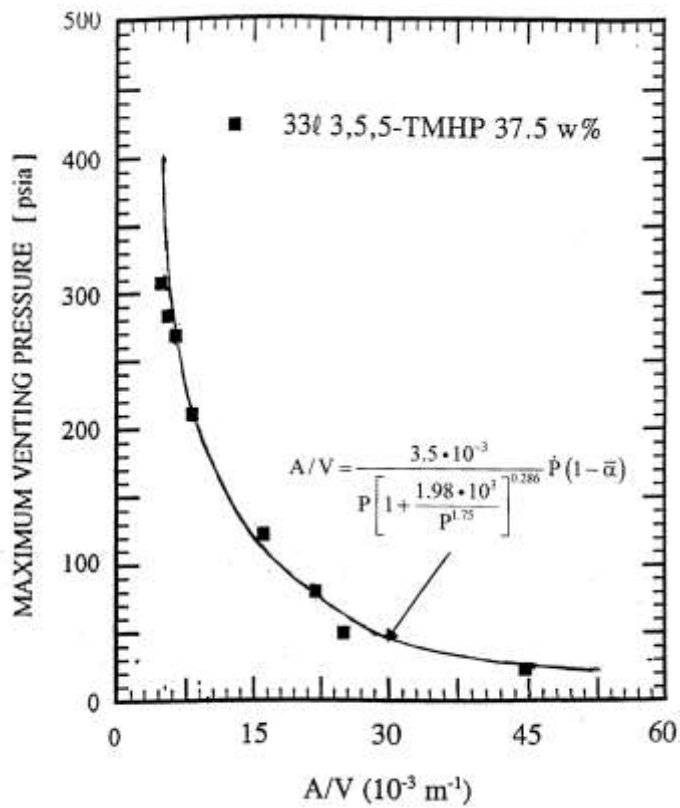


Figure 4. Comparison Between Predictions and Experimental Data

The noted decrease in average void fraction,  $\bar{\alpha}$ , as the peak pressure increase is as it should be, i.e., the transit mass loss effect decreases with increasing pressure.

The above effect on the vent size can be estimated from Fauske's generalized sizing equation applied to gassy systems as follows:

$$A/V = \frac{3.5 \times 10^{-3}}{P \left[ 1 + \frac{1.98 \times 10^3}{P^{1.75}} \right]^{0.286}} \dot{P} (1 - \bar{\alpha}) \quad (23)$$

where

$A$  ( $\text{m}^2$ ) = vent area,

$V$  ( $\text{m}^3$ ) = vessel volume,

$\dot{P}$  ( $\text{psi min}^{-1}$ ) = peak pressure rise in RSST containment volume with 10 g sample,

$P$  (psig) = peak venting pressure, and

$\bar{\alpha}$  = average void fraction determined from Eq. 22.

Predictions from Eq. 23 are illustrated in Figure 4 indicating good agreement with the experimental data.

The above suggested approach to account for transient mass loss effect is also confirmed by available large-scale venting tests with neat dicumyl peroxide [10]. A 58 gallon test vessel with an effective vent diameter of 10.9 inches filled with neat dicumyl peroxide ( $A/V = 0.27$ ), vented safely with a peak pressure of about 5 psig. Applying Eq. 22 with  $V = 0.22 \text{ m}^3$ ,  $A_{\text{vessel}} = 0.26 \text{ m}^2$ ,  $\rho_{\ell} = 1000 \text{ kg m}^{-3}$  and  $u_{\infty} = 0.2 \text{ m s}^{-1}$  along with RSST information of  $m_t = 0.01 \text{ kg}$ ,  $v = 3.5 \cdot 10^{-4} \text{ m}^3$ ,  $\dot{P} = 71.7 \text{ psi s}^{-1}$  and a peak relief pressure  $P = 20 \text{ psia}$ , results in  $\bar{\alpha} \approx 0.66$ , and from Eq. 23

$$\begin{aligned} A/V &= \frac{3.5 \times 10^{-3}}{5 \left[ 1 + \frac{1.98 \times 10^3}{5^{1.75}} \right]^{0.286}} \times 4300 (1 - 0.66) \\ &= \underline{0.26 \text{ m}^{-1}} \end{aligned}$$

which is consistent with the experiment value of  $\underline{0.27 \text{ m}^{-1}}$ .

A full scale 460 gallon test vessel with a vent diameter of 22.5 inches filled with neat dicumyl peroxide ( $A/V = 0.14$ ) vented safely with a peak relief pressure of 20 psig. Again, applying Eq. 22 for these conditions results in  $\bar{\alpha} \approx 0.66$ , and applying Eq. 23

$$\begin{aligned} A/V &= \frac{3.5 \times 10^{-3}}{20 \left[ 1 + \frac{1.98 \times 10^3}{20^{1.75}} \right]^{0.286}} \times 4300 (1 - 0.66) \\ &= \underline{0.13 \text{ m}^{-1}} \end{aligned}$$

which is consistent with the experiment value of  $0.14 \text{ m}^{-1}$ . Considering that uncertainties may exist in predicting the transient mass loss for a given system, it is recommended that the  $(1 - \bar{\alpha})$  term in Eq. 23 is set equal to the initial vessel fill fraction.

### 3.1 Gassy System Design Example

For some runaway reaction systems the peak reactivity rate also depends upon the prevailing pressure. This is the case for the tributyl phosphate-HNO<sub>3</sub> system, where data suggest that the peak reactivity rate is directly proportional to the pressure. Eq. 23 can be stated as

$$A/V = \frac{3.5 \times 10^{-3}}{P \left( 1 + \frac{1.98 \times 10^3}{P^{1.75}} \right)^{0.286}} P^1 \quad (24)$$

where  $P^1$  (psia) =  $P + 14.7$ . When critical flow prevails, this implies that the peak volumetric gas generation rate or the A/V ratio is invariant with pressure. Predictions from Eq. 24 are in excellent agreement with both highly subcritical and critical flow VSP vented test results as illustrated in Table 4.

Table 4. Comparison Between Vented VSP Tests and Eq. 24 Predictions

Venting Pressure P, psig	(A/V) <sub>exp</sub> m <sup>-1</sup>	(A/V) <sub>Eq. 24</sub> m <sup>-1</sup>
0.3	0.0106	0.0109
9.6*	--	0.0031
22	0.0032	0.0031
200	0.0032	0.0034
* Corresponds to critical flow for isothermal condition.		

An example of bad and good design practices is illustrated in Table 5 for this organic nitric acid system in a vessel with a MAWP of 30 psig.

Table 5. Example of Design Practices

Design Practice	Relief Set Pressure	(A/V) <sub>Eq. 24</sub>
Bad	= MAWP = 30 psig	0.0031 m <sup>-1</sup>
Good	= 2 psig	0.0047 m <sup>-1</sup>

Following the good practice by selecting a subcritical relief set pressure eliminates the extreme sensitivity to pressure by being slightly off in the peak reactivity rate, recalling the latter property is directly proportional to the venting pressure.

## **4. HYBRID SYSTEMS**

For systems where both gaseous reaction products and vapor pressure can play a role, effective tempering of the chemical reaction due to latent heat of vaporization can occur well before reaching the peak volume generation rate. Again, in the absence of experimental hybrid venting data at the time, the DIERS methodology suggested a conservative approach (worst case) by assuming two-phase homogeneous venting coinciding with onset of tempering [1]

$$A = \frac{(\dot{Q}_g + \dot{Q}_v) \rho_\ell (1 - \alpha)}{G} \quad (25)$$

where

$A$  ( $\text{m}^2$ ) = vent area based on homogeneous two-phase flow,

$\dot{Q}_g$  ( $\text{m}^3 \text{s}^{-1}$ ) = gas volume generation rate at tempering,

$\dot{Q}_v$  ( $\text{m}^3 \text{s}^{-1}$ ) = vapor volume generation rate at tempering,

$\rho_\ell$  ( $\text{kg m}^{-3}$ ) - reactant density,

$\alpha$  = initial free board volume,

and  $G$  ( $\text{kg m}^{-2} \text{s}^{-1}$ ) is the homogeneous gas-vapor-liquid flow rate given by

$$G \sim \sqrt{2 P_g \rho_\ell + G_{\text{ERM}}^2} \quad (26)$$

where  $P_g$  (Pa) is the partial pressure of gas and  $G_{\text{ERM}}$  ( $\text{kg m}^{-2} \text{s}^{-1}$ ) is the equilibrium rate model flow rate evaluated at the appropriate vapor pressure. Again, the augmentation in vent size relative to all gas-vapor venting will be large and in contrast to vapor systems, allowing for a modest overpressure will not significantly reduce this difference. Here again it is appropriate to quote the 1983 DIERS technology report [1] "similar to pure gas generating systems early two-phase venting has the potential of reducing the vent size relative to that predicted from Eq. 25".

Extensive venting experience has since become available for the hydrogen peroxide (HP) hybrid system indicating an order of magnitude smaller venting requirement than suggested by Eq. 25. The following totally empirical approach, based upon the analysis of post hydrogen peroxide incidents

$$200 \text{ cm}^2/\text{tonne H}_2\text{O}_2 \text{ 100\%} \quad (27)$$

is commonly used for the design of the relief vent by the users of HP, and is considered adequate for contamination factors as high as of the order of 1000 [11]. Setting the density of 100%  $\text{H}_2\text{O}_2$  equal to  $1400 \text{ kg m}^{-3}$  condition (27) can be restated as

$$A/V = 2.8 \times 10^{-2} \text{ m}^{-1} \quad (28)$$



where  $A$  ( $m^2$ ) is the vent area and  $V$  ( $m^3$ ) is the volume of 100% HP.

It is of interest to compare the above venting requirement to Eq. 25 and Fauske's generalized sizing equation applied to hybrid systems

$$A/V = \frac{3.5 \times 10^{-3}}{P \left[ 1 + \frac{1980}{P^{1.75}} \right]^{0.286}} (\dot{T} + \dot{P}) \quad (29)$$

where

$A$  ( $m^2$ ) = vent area,

$V$  ( $m^3$ ) = volume of HP solution,

$P$  (psig) = relief set pressure,

$\dot{T}$  ( $^{\circ}C \text{ min}^{-1}$ ) = self heat rate at tempering,

$\dot{P}$  ( $\text{psi min}^{-1}$ ) = rate of pressure rise at tempering in the RSST containment volume with 10 g sample.

Considering the following example of 907 kg 25% wt  $H_2O_2$  with a relief set pressure (tempering condition) of 5 psig and corresponding RSST measurements of  $\dot{T} = 23^{\circ}C \text{ min}^{-1}$  (contamination factor of the order of 1000) and  $\dot{P} = 6 \text{ psi min}^{-1}$  (10 g RSST sample). Applying this example to Eq. 25 considering 20% overpressure results in<sup>5</sup>

$$A = 550 \text{ cm}^2$$

This compares to condition (27 or 28) of

$$A = 45 \text{ cm}^2$$

and from Eq. 29 of

$$A = 46 \text{ cm}^2$$

i.e., the assumption of onset of homogeneous two-phase flow at the tempering condition (Eq. 25) overpredicts the vent size by an order of magnitude compared to the extensive experience with the hydrogen peroxide system. The noted large difference between Eq. 25 and Eq. 29 results from the all gas-vapor venting approach used to develop Eq. 29 which is consistent with experimental observations (runaway with 200 kg 50% wt  $H_2O_2$  solutions) [6].

#### **4.1 Hybrid System Design Example**

An experiment with a 200 kg 50%  $H_2O_2$  solution with a contamination factor of about 3500 is used here to illustrate preferred design practice [6]. The runaway reaction tempered and vented safely with a value of  $A/V = 2.6 \times 10^{-2} \text{ m}^{-1}$  and a resulting relief

---

<sup>5</sup> Leung's more detailed hybrid system solution results in  $A = 516 \text{ cm}^2$  [12].

pressure of about 1 psig. The self-heat rate at tempering equaled  $55^{\circ}\text{C min}^{-1}$  and the inferred rate of pressure rise was  $14 \text{ psi min}^{-1}$  (corresponding to a 10 g sample in the RSST).

In this case the preferred design practice is the use of Eq. 29

$$\begin{aligned} A/V &= \frac{3.5 \times 10^{-3}}{1 \left[ 1 + \frac{1.98 \times 10^3}{1^{1.75}} \right]^{0.286}} (55 + 14) \\ &= 2.75 \times 10^{-2} \text{ m}^{-1} \end{aligned}$$

which compares to the experimental value of  $2.6 \times 10^{-2} \text{ m}^{-1}$ . In this case due to the high contamination factor, the use of the hydrogen peroxide Bulk Storage Guidelines (condition 27) underestimates the venting requirement by a factor of 2 ( $A/V \sim 1.4 \times 10^{-2} \text{ m}^{-1}$ ) while the original DIERS methodology (Eq. 25) overestimates the venting requirement by an order of magnitude ( $A/V \sim 3 \times 10^{-1} \text{ m}^{-1}$ ).

## **5. CONCLUDING REMARKS**

The original DIERS methodology for vapor systems captured the dramatic decrease in the vent size with overpressure considering two-phase flow. Changing the often common practice of setting the relief pressure equal to MAWP to a lower practical setting, the noted overpressure effect allows vent sizing based upon all vapor venting for non-foamy systems and twice the all vapor venting area for foamy systems.

Due to lack of relevant experimental data, the original DIERS methodology included conservative modeling of gassy systems (including hybrid systems) based upon initiation of homogeneous two-phase flow coinciding with the peak reactive condition. Limited experimental data have since become available that support vent sizing based upon all gas venting at the peak reactive condition with no prior reactant loss, resulting in an order of magnitude decrease in the venting requirement. This is an area where additional gassy (including hybrid) system data are needed to further clarify the role of two-phase flow.

## **6. REFERENCES**

1. Fauske & Associates, Inc., 1983, "Emergency Relief Systems for Runaway Chemical Reactions and Storage Vessels: A Summary of Multiphase Flow Methods," FAI/83-27, October 1993.
2. Fisher, H. G., et al., 1992, "Emergency Relief System Design Using DIERS Technology," AIChE, New York, NY.
3. Fauske, Hans K., 2003, "Generalized Vent Sizing Equation for Reactive Systems," FAI Process Safety News, Summer 2003.
4. Fauske, H. K. et al., 1986, "Emergency Relief Vent Sizing for Fire Emergencies Involving Liquid-Filled Atmospheric Storage Vessels," Plant/Operation Progress, Vol. 5, No. 4, 1986.
5. Grolmes, M. A. and Epstein, M., 1985, Plant/Operation Progress, October, 1985.
6. Wilberforce, J. K., 1988, "Emergency Venting of Hydrogen Peroxide Tanks," CEFIC Hydrogen Peroxide Safety Conference, Gothenburg, Sweden, Sept. 22, 1988.
7. Fauske, H. K., 2000, "Properly Size Venting for Nonreactive and Reactive Chemicals," Chemical Eng. Progress, February, 2000.

8. Epstein, M., Fauske, H. K. and Hauser, G. M., 1989, "The Onset of Two-Phase Venting via Entrainment in Liquid-Filled Storage Vessels Exposed to Fire," *J. Loss Prev. Process Ind.* 2 (1), p. 45, 1989.
9. Fauske, H. K., 1999, "Determine Two-Phase Flows During Releases," *Chemical Engineering Progress*, February 1999.
10. Fauske, Hans K., 2004, "Gassy System Vent Sizing - the Role of Two-Phase Flow," *FAI Process Safety News*, Fall 2004.
11. Fauske, Hans K., 2005, "Tools for Assessing Hydrogen Peroxide (HP) Stability and Storage Vents," *FAI Process Safety News*, Spring 2005.
12. Leung, J. C., 1992, "Venting of Runaway Reactions with Gas Generation," *AIChE Journal*, Vol. 38, No. 5, May 1992.